Technology Advances and Challenges in Hermetic Packaging for Implantable Medical Devices

Guangqiang Jiang and David D. Zhou

Abstract Many implantable medical devices contain sophisticated electronic circuits. Hermetic packaging is required to provide the implant's electronic circuitry with protection from the harsh environment of the human body. This chapter provides a review of available hermetic sealing methods and their applications. General considerations of implantable medical device packaging are discussed. Various testing methods applicable to the packaging of implantable medical devices are also presented. Many issues associated with hermetic packaging are not yet completely understood, nor are any corresponding difficulties completely overcome. The continued miniaturization of future implantable medical devices provides both opportunities and challenges for packaging/materials engineers to improve the existing packaging methods, and to develop new methods. Reliable hermetic micropackaging technologies are the key to a wide utilization of microelectromechanical systems (MEMS) in miniaturized implantable medical devices.

Contents

1 Introduction 28
1.1 Hermetic Packaging Technology Advances 28
1.2 Significance of Hermetic Packaging for Implantable Medical Devices 31
2 General Packaging Considerations for Implantable Medical Devices 31
2.1 Biocompatibility 31
2.2 Hermeticity Requirement 32
2.3 Outgassing of Internal Materials 32
2.4 Wireless Communication 33
2.5 Package Heating 33
2.6 Coefficient of Thermal Expansion Compatibility 33

G. Jiang (✉)
Alfred E. Mann Foundation for Scientific Research, Santa Clarita, CA 91355, USA
e-mail: jiang@aemf.org

D.D. Zhou, E. Greenbaum (eds.), *Implantable Neural Prostheses 2*,
Biological and Medical Physics, Biomedical Engineering, DOI 10.1007/978-0-387-98120-8_2,

3 Types of Hermetic Sealing and Their Applications 34
3.1 Polymer Encapsulation 34
3.2 Glass-to-Metal Seal 34
3.3 Ceramic-to-Metal Feedthrough 35
3.4 Ceramic-to-Metal Seal 37
3.5 Hermetic Seal with Fusion Welding 39
3.6 Conductive Vias on Ceramic Substrate 40
4 Testing Methods for Hermetic Sealing of Implantable Medical Devices 41
4.1 Mechanical and Environmental Tests 41
4.2 Hermeticity Testing Methods and Their Limitations 42
4.3 Biocompatibility Tests 45
4.4 Corrosion Tests 46
4.5 Morphological and Microstructural Characterization 47
4.6 Accelerated Life Test 48
4.7 X-Ray Microscopy 49
4.8 Acoustic Microscopy 51
5 Challenges of Hermetic Packaging for Implantable Medical Devices 51
5.1 Long-Term Stability of Ceramic Materials 51
5.2 Metals and Alloys Corrosion 52
5.3 Challenges in Accelerated Life Test 53
5.4 Hermeticity Test Reliability for Miniature Devices 54
5.5 Design challenges for Miniature Devices 55
5.6 Hermetic Packaging of MEMS for Implantable Medical Devices 55
6 Conclusions 56
References 56

1 Introduction

Implantable medical devices have been widely used to restore body functions, improve the quality of life, or save lives. Experts estimate that 8 to 10 percent of all Americans (some 20 million to 25 million people) [1], or about 1 in 17 people in industrialized countries [2], carry some form of implanted device. Many medical devices, such as the implantable cardiac defibrillator, cochlear implant, artificial vision prosthesis, neuromuscular microstimulator, and the like contain sophisticated electronic circuits. Such long-term implantable medical devices are susceptible to damage by body fluids over time. Hermetic packaging is required to protect the electronic circuitry of the implant from the harsh environment of the human body.

1.1 Hermetic Packaging Technology Advances

There are a variety of ways to define hermeticity. Webster's New Collegiate Dictionary defines hermeticity as "the state or condition of being airtight," or in the Microelectronics Packaging Handbook [3], it is defined as "sealed so that the

object is gas tight." In the real physical world, there is no such thing as absolute or complete hermeticity because all materials are gas permeable to some degree [4].

The packaging of implantable medical devices uses various materials, including polymers, glasses, metals, and ceramics. The encapsulation method used is greatly dependent upon the technology of the electronic circuit that is to be encapsulated. Polymer encapsulation has been successfully used with relatively simple circuits assembled from discrete, low-voltage components [5]. With polymer encapsulation, the discrete components are often compactly arranged and "potted" in a mold with leads or conductive feedthrough pins penetrating through the polymeric encapsulation wall [6]. This has historically been the preferable approach to encapsulation because of its simplicity and relatively low processing temperature; however, polymers do not provide an impermeable barrier. Moisture ingress will ultimately reach the electronic components, and surface ions can allow electric shorting and degradation of the leakage-sensitive circuitry and subsequent failure of the device [7]. Therefore, in general, polymer encapsulation is unsuitable for high-density, high-voltage electronics circuits. Recent research on liquid crystal polymers (LCPs) would suggest that using LCPs for near-hermetic packages in implantable medical devices looks promising [8, 9].

Hermeticity of early experimental cochlear implants used the principles of mechanical pressure and gasket sealing [10]. Though the human implanted system permitted changes from percutaneous cable to transcutaneous telemetry for the first time, no report on the long-term performance of such a sealing mechanism used in this implant has been issued. Materials that may provide a hermetic barrier are metals, ceramics, and glasses. Metallic packaging generally uses a biocompatible metal capsule that is either machined from a solid piece of metal or deep drawn from a piece of sheet metal. Electrical signals enter and exit the package through hermetic feedthroughs. The feedthrough assembly often utilizes a ceramic or glass insulator to allow one or more conducting wires to exit the package without coming in contact with the package itself. This method has been successfully used for implantable pacemakers [11], cardioverter defibrillators [12], implantable multichannel neuromuscular stimulators [6], and cochlear implants [13].

Metal-based packaging generally requires that a power-receiving coil or communication antenna be placed outside the package to avoid significant loss of power or radio frequency signals through the walls of the implanted device, thus requiring additional space within the body to accommodate the volume of the entire implant. Bioceramics and biograde glasses possess a radio frequency transparency advantage over metallic materials. They have been used as the main packaging materials for the implantable neuromuscular microstimulators [14, 15], cochlear implants [16], and artificial retina implants [17]. Bioceramics used for structural applications include alumina (both single crystal sapphire and ruby or polycrystalline α–Al_2O_3) [18–22], zirconia (magnesium oxide partial stabilized zirconia (Mg-PSZ)) [23], yttria-stabilized tetragonal zirconia polycrystals (Y-TZP) [23], and ceria stabilized zirconia poly-crystal (Ce-TZP) [24–29]). Many different types of biocompatible glass have been successfully used for implantable medical devices,

including borosilicate glass (Kimbel N51A) for the glass capsule neuromuscular microstimulator [14].

A conductive component is often the required interfacial material for an active implantable medical device for the purposes of sensing and delivering electrical signals from/to living tissue. Though the main body of the package is made of bioceramic or biocompatible glass, hermetic bonding between the ceramics or glasses and metallic/conductive components is essential. To enable a hermetic seal between similar or dissimilar metallic components, fusion welding methods, such as laser welding, tungsten inert gas welding (TIG), and electron-beam welding, are often the choices. Figure 1 shows three neuromuscular microstimulators (BIONs) in different packages. The AMI glass-packaged neuromuscular microstimulator contains three hermetic seals: two glass-to-tantalum seals produced by melting glass with an infrared laser beam; and one final hermetic seal that is obtained by melting the tantalum tube closed in a plasma needle arc welder [14]. Metal-to-ceramic brazed cases provided housing for both the AMF and ABC neuromuscular microstimulators [30–32] and the final hermetic seals were achieved by a laser-welding method.

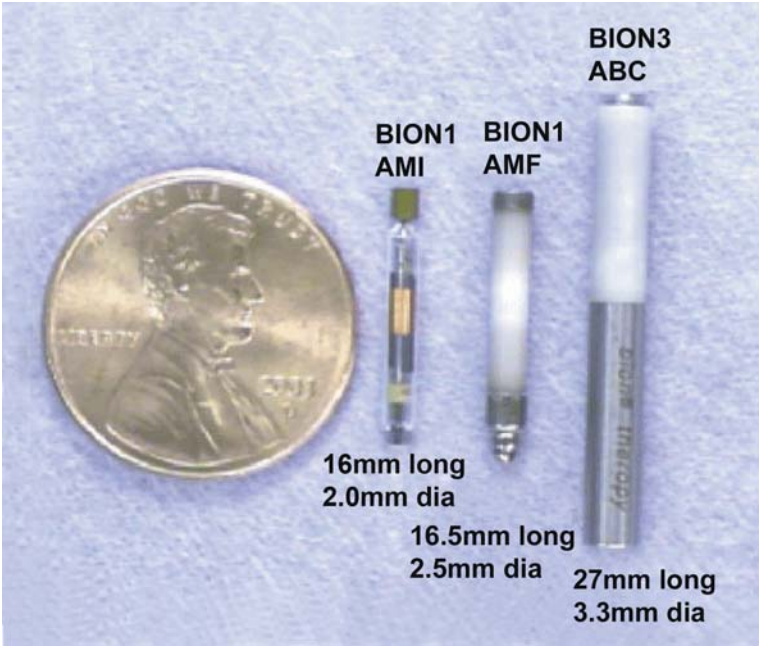

Fig. 1 Photograph depicting three neuromuscular microstimulators (BIONs) in different packages. The diameters of three BIONs are 2.0 mm from AMI-Alfred Mann Institute at University of Southern California, 2.5 mm from AMF – Alfred Mann Foundation, and 3.3 mm from ABC – Advanced Bionic Corp. (Reprinted from [33] with permission of the American Association of Neurological Surgeons)

1.2 Significance of Hermetic Packaging for Implantable Medical Devices

Despite the multitude of designs for implantable medical devices, there are usually four integral parts that must be accounted for: (1) the input or sensor, (2) the lead and lead connections, (3) the main package body, and (4) the output [34]. The principle failure points for these implant devices occur at the interfacial boundaries of adjoining surfaces, where water and ion migration proceed along the lead connections [7]. For example, an auditory reliability report, issued in 2006 by a medical device company, disclosed that roughly three out of four device failures were attributed to moisture ingression into the titanium receiver-stimulator packaging of an implant through the feedthrough (available online at http://www.bionicear.com/printables/reliabilityreport2006.pdf, accessed 10 January 2008). Water penetrating the intact polymeric encapsulants and permeating to the underlying substrates [35] is also a common cause of failure. Moisture ingress can result in failures such as open circuits [36], damage to metallics [36], surface electrical leakage [37], and electrical shorts due to moisture-promoted dendritic growth of silver and gold [37–39]. Ingress of other active gases, such as oxygen, could also cause attachment failure of solder-attached components due to solder oxidization [40].

This chapter provides a review of the available hermetic packaging methods and their applications. This has been a difficult task, as manufacturers of medical devices do not usually disclose the details of their packaging methods to protect their competitive edge. Many implantable medical devices have utilized one or more of the hermetic packaging methods. General considerations of packaging and testing methods for implantable medical devices are discussed in this chapter. Challenges associated with further advancement of implantable medical devices and future directions in the field are also examined.

2 General Packaging Considerations for Implantable Medical Devices

2.1 Biocompatibility

Biocompatibility is the first thing that the packaging engineer should consider when designing a hermetic package for an implantable medical device, as it is the package that makes direct contact with body tissue. It is critical that implantable medical devices do not elicit any undesirable local or systemic effects in the human body. In addition, the package materials should be stable and must be able to withstand attack from a harsh ionic body environment.

Biocompatible materials that have been successfully used for implantable medical device packaging include titanium and its alloys, noble metals and their alloys, biograde stainless steels, some cobalt-based alloys, tantalum, niobium, titanium-niobium alloys, Nitinol, MP35N (a nickel-cobalt-chromium-molybdenum alloy),

alumina, zirconia, some biocompatible glass and polymers. A series of biocompatibility testings often suggested by the Food and Drug Administration (FDA) will be discussed in Section 4.3

2.2 Hermeticity Requirement

The degree and measure of hermeticity are a function of material choice, final seal design, fabrication processes and practices, and the use environment; so, before deciding what kind of packaging method to select for the implantable medical device, one needs to consider the level of hermeticity that is needed and the life span expectations for the product. Theoretically, all materials and all welded or joined assemblies will leak to some degree [4], whether by permeation through the bulk material or along a discontinuity path. The property of the solid that characterizes the amount of gas that can pass though the solid is called permeability [41]. The function of permeability is a combination of mass (g), distance (cm), time (s), and pressure (torr). Standard engineering practice would graph the permeability function as g/cm-s-torr. Figure 2 shows the typical helium permeability of many common classes of packaging materials and their predicted lifetime at different thicknesses. As mentioned previously, polymeric materials do not provide an impermeable barrier. Thus glasses, ceramics, metals, and single crystals can be considered for long-term implants.

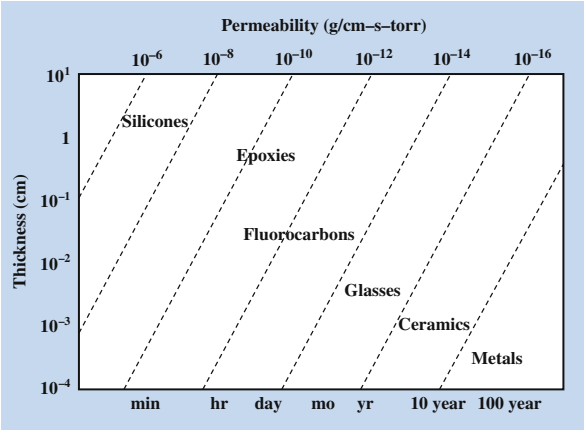

Fig. 2 Permeability chart for common classes of packaging materials (Reprinted from [4] with permission of Medical Device and Diagnostic Industry. Copyright © 2000 Canon Communications LLC)

2.3 Outgassing of Internal Materials

Even if the package materials and the sealing process(es) effectively prevent leakage through the package wall, implants still fail in some cases. The internal materials in a package, such as silicones, epoxies, and polymer coatings or insulators for chips and discrete electrical elements, often outgas which increases the vapor pressure and

moisture level inside the package. The internal outgassing may induce the formation of water droplet condensation, thus compromising the device performance and eventually leading to device failure. Control of these internal sources of contaminants is essential to guarantee long-term reliability.

2.4 Wireless Communication

Wireless communication between the implantable medical device and external control unit eliminates the need for percutaneous wires, so that the risk of infection can be minimized. In some cases, the receiving coils are placed outside the metallic hermetic package and then jointly embedded with the metallic packaging using polymer encapsulation. The received signal can then be transmitted to the electronic circuitry inside the metallic package by utilizing feedthrough pins. In a polymer-encapsulated coil design, there is an issue that must be addressed: altering the inductance of the receiving coil, due to moisture ingress at the coil interface, causes the quality factor Q to decrease, thereby lowering the gain of the stage. Bioceramics and biocompatible glass provide a transparent radio frequency window for wireless communication. By employing bioceramic or biocompatible glass as the packaging material, the receiving coil can be placed inside the package and wireless communication can be established through the package.

2.5 Package Heating

When a metallic material is used as the main package body, problems such as metal heating have to be considered. As noted above, metallic materials attenuate electromagnetic and radio frequency signals. To provide reliable communication and effective charging to the implanted receiving coils encapsulated in the metallic package, strong electromagnetic signals from external transmitters are required. Eddy currents generated inside the metallic bulk generate heat when an electromagnetic field is present. International standard ISO 14708-1:2000 E requires that no outer surface of an implantable part of the active implantable medical device shall be greater than 2°C above the normal surrounding body temperature of 37°C when implanted, and when the active implantable medical device is in normal operation or in any single-fault condition. Special consideration must be given to the amount and types of metallic materials and to the package design for the implanted device to avoid excessive heating.

2.6 Coefficient of Thermal Expansion Compatibility

When bonding dissimilar materials, especially those involving high-temperature processes such as brazing or welding, a coefficient of thermal expansion (CTE) compatibility between the parts to be joined has to be considered. The larger the CTE mismatch and the bigger the parts, the higher the possible residual stress in the

assembly. Such residual stress can result in failure, such as cracking, or can compromise the hermeticity of the assembly. Sometimes the failures may not appear immediately, and the consequences can be worse when discovered later. Early versions of the AMI neuromuscular stimulator package used a tubular feedthrough of 90% Pt–10% Ir. The seals produced were hermetic initially, but tended to fail catastrophically during prolonged soaking and temperature cycling in saline because of the difference in the CTE between the glass capsule wall (5.5×10^{-6}/°C) and the 90% Pt–10% Ir feedthrough (8.7×10^{-6}/°C). The excess residual stress in the walls of the sealed glass capsules can be measured using the photoelastic effect on the rotation of polarized light (Model 33 Polarimeter, Polarmetrics, Inc., Hillsborough, NH) [14]. By using tantalum (CTE = 6.5×10^{-6}/°C) as the feedthrough material, the residual stress is reduced.

3 Types of Hermetic Sealing and Their Applications

3.1 Polymer Encapsulation

There are numerous organic polymeric materials that are used as encapsulants for electronics. These materials are divided into (1) thermosetting polymers, (2) thermoplastics, and (3) elastomers. For implantable medical device applications, only a few materials in the above three groups can be made ultrapure to serve as acceptable encapsulations for implants [42]. Candidate materials include epoxies, silicones, polyurethanes, polyimides, silicone-polyimides, parylenes, polycyclicolefins, silicon-carbons, and benzocyclobutenes, as well as recently developed high-performance liquid crystal polymers (LCPs). Silicone rubber has been used as cable insulation material [43], epoxies were used in part for electronic component encapsulation [44], and Parylene C is utilized as an insulation coating on electronics in implants [45, 46]. The challenge of polymer encapsulations when applied to a long-term biomedical device primarily lies in their bio-stability within the body. Degradation of polymers includes hydrolytic, oxidative, and enzymatic mechanisms that deteriorate the chemical structure [47]. Polymer encapsulation has been successfully used with relatively simple circuits using discrete, low-voltage components. However, polymer encapsulation does not provide an impermeable barrier [48] and therefore cannot be used for packaging high-density, high-voltage electronic circuitry for long-term applications.

3.2 Glass-to-Metal Seal

Glass-to-metal seal technology is used extensively to provide a hermetic seal between a metal conductor and a metal body. Hermeticity of a glass-to-metal seal can typically be 1×10^{-8} standard cubic centimeters of gas at a pressure of one

atmosphere per second (atm-cc/sec) or less, as measured by the helium-leakage rate. A typical glass-to-metal seal consists of the following elements:

- A metal bulkhead (or body) with a hole or holes in it.
- A pin(s) serving as a conductor(s) in the center of this hole(s).
- A piece of glass preformed to fit between the pin(s) and the bulkhead.

During processing, these three components are placed on a fixture which holds them in position. The entire assembly is then heated in a controlled atmosphere to the appropriate temperature for the particular set of materials. At the sealing temperature, the glass melts and fills the space between the pin and the bulkhead, and a hermetic seal is formed upon cooling.

The type of seal generated by this process is dependent upon the type of glass used and the materials used for the bulkhead and pins; there are two basic types of seals, the compression seal and the reactive seal. Early cochlear implants had used a compression glass-to-metal seal to form feedthroughs to provide the connection for 16 electrodes. Sixteen pure platinum feedthrough pins are precisely placed in position in a polycrystalline glass-ceramic substrate with a commercially pure (CP) Ti ring on the outside. The polycrystalline glass-ceramic has slightly smaller CTE than CP Ti. Upon cooling, the CP Ti ring shrinks and squeezes the glass onto the pure platinum pins to form a strong compression seal.

This reactive seal was the choice of the first-generation neuromuscular microstimulator [14]. The hermeticity of the glass-to-metal seals depends on chemical bonding between the borosilicate glass (Kimble N-51A®) and the native oxide on the tantalum electrode stem and the tantalum tubular feedthrough. Enclosures with this type of glass-to-metal seal may experience a transient loss of hermeticity and ingress of ambient gases when subjected to mechanical pressure. Integrity of glass-to-metal seals depends on a strong bond of glass-to-metal oxide at the metal/glass interface. If this bond is weakened, or otherwise compromised by inadequate oxide thickness or contamination, the seals may temporarily give way during slight distortions of the package by mechanical pressures of fixturing the unit for testing, e.g., centrifuge or fine/gross leak. Although glass-to-metal seals can be initially hermetic, their performance after temperature cycling is of suspect [14, 49]. Graeme reported that fluids and enzymes can permeate along minute pathways, or open up cracks in the glass seals through surface tension, and this was one failure mode of the early University of Melbourne's cochlear implant prototypes seen in two of the three initial patients [50].

3.3 Ceramic-to-Metal Feedthrough

A properly produced ceramic-to-metal feedthrough seal is often more robust, more durable, and has tighter hermeticity and better electrical insulation than a glass-to-metal feedthrough seal. Ninety-two percent or higher purity alumina as well as

100% pure sapphire and ruby are commonly used for hermetic seal of implantable medical devices. Other ceramics such as aluminum nitride (AlN), zirconia (ZrO_2), silicon carbide (SiC), and silicon nitride (Si_3N_4) have the potential to be used for ceramic-to-metal assemblies for implantable medical devices.

Properly designed ceramic-to-metal feedthrough seals are able to maintain hermeticity in a variety of harsh conditions, such as temperature cycling, corrosive, thermal shock, and varying pressure environments. Ceramic functions as an excellent electrical insulator at elevated temperatures, unlike glass, which conducts more electricity at high temperatures. Moreover, ceramics are less likely to fracture when subjected to high-vibration and high-acceleration conditions than glass. An additional problem for glass is the tendency of meniscus formation at the surface leading to small pieces breaking off – obviously an undesirable situation for medical implants.

Applications of ceramic-to-metal feedthroughs for implantable medical devices include implantable pacemakers [11], cardioverter defibrillators [12], implantable multichannel neuromuscular stimulator [6], and cochlear implants [16]. One commonly used ceramic-to-metal feedthrough in the implantable medical device applications is a pure platinum pin(s) in an alumina substrate [51], as illustrated in Fig. 3. This feedthrough assembly can be produced either with sputtered 99.99% gold brazing or by co-fire pure platinum pins with green alumina ceramic. In the case of brazing, a thin film of metal such as gold, platinum, niobium, or titanium can be applied on the ceramic via physical vapor deposition (PVD) to promote adhesion [52]. Insulation materials (typically silicone and polyurethane) are usually applied on the ceramic-to-metal interface (to prevent shorting due to moisture-promoted dendritic growth of gold) and between pins (to isolate the conductor).

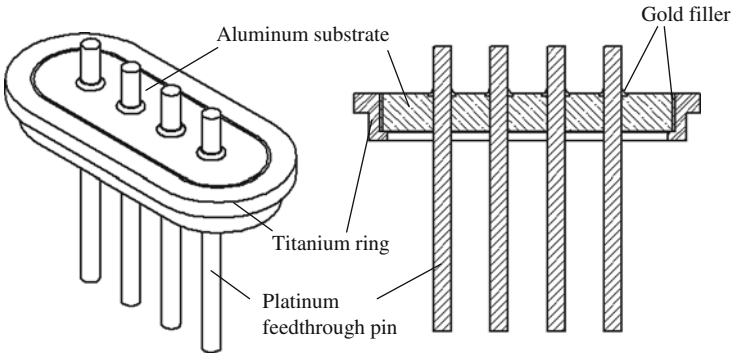

Fig. 3 A ceramic-to-metal implantable feedthrough

Section 3.4 will discuss in detail the investigation of different types of bonding methods (including active brazing, nonactive brazing, and diffusion bonding) aimed at producing hermetic ceramic-to-metal seals for implantable medical device applications. The fundamentals are applicable to the ceramic-to-metal feedthrough design as well.

3.4 Ceramic-to-Metal Seal

Sometimes a ceramic-to-metal seal is the preferable design, as in the AMF neuromuscular microstimulator, where no feedthrough pin is needed. Pure iridium and platinum-iridium components attached to the titanium metal parts act as electrodes interfacing with living tissue.

Brazing is by far the most widely used joining process for a ceramic-to-metal seal when mechanically reliable hermetic joints are required. Brazing is a process for joining two or more solid materials in close proximity to each other by introducing a filler material that melts at a high temperature (typically above 450°C) and which is below the melting points of the materials being joined. Filler materials are classified into two categories: active and nonactive. Active fillers are composed of chemically active materials or compounds that convert readily and permanently from one composition to another when subjected to sufficient energy to initiate the reaction. For the purposes of this discussion, the active fillers to be considered are often composed of active elements, such as titanium, aluminum, hafnium, zirconium, vanadium, and niobium, and the energy applied to initiate the conversion is heat. Nonactive filler materials often require prior metallization of the ceramic substrate to provide for enough wetting, so an interface (usually reactive) is formed. Physical vapor deposition (PVD), chemical vapor deposition (CVD), or mechanical metallization can be used to deposit metallic films, such as molybdenum, manganese, tungsten, or their combination onto ceramic surfaces prior to brazing. This additional metallization step can complicate the brazing process and makes quality control of the joint more difficult. Brazing with active filler materials is a relatively simple method and is generally preferred over brazing with nonactive fillers.

3.4.1 Active Brazing

Both zirconia and titanium have been widely used for biomedical applications due to their excellent mechanical properties and favorable biocompatibility [23, 30]. It is desirable to bond these two materials together for some applications [30]. Some earlier studies have selected active filler alloy brazing as the joining technique for zirconia to Ti-6Al-4 V and have successfully brazed the zirconia to Ti-6Al-4 V with Ag-Cu series filler materials [53–55]. Although this method seems very promising in terms of interfacial strength, it might meet with some objections regarding biomedical applications and the possible toxicity of Cu. Lasater disclosed a method to produce hermetically sealed zirconia-to-titanium joints using a titanium-nickel alloy filler material [56]. Fey and Jiang discovered that zirconia could be joined to titanium alloys using pure nickel brazing filler material [57]. In such a case, the titanium element from the base metal diffuses with nickel filler material and reacts to form a eutectic alloy at the interface. The Ni_2Ti_4O phase that formed upon cooling at the ceramic-to-metal interface is responsible for the bond development. Jiang et al. reported that the zirconia-to-Ti-6Al-4 V brazed joints have good biocompatibility and have been successfully used for the second-generation neuromuscular microstimulators developed at the Alfred Mann Foundation, Santa Clarita, California, USA

[30]. Other successful examples of ceramic-to-metal packages include alumina to Ti-45%Nb alloy package brazed with TiNi-50® active filler metal, for cochlear implant application; alumina to pure niobium case bonded with TiNi-50® filler metal, also for cochlear implant; and alumina to a metal assembly brazed with a modified active filler metal, for artificial retina packaging.

3.4.2 Nonactive Brazing

3.4.2.1 Metalized Ceramic Brazing

By metalizing the surface of the ceramic to be joined by depositing or embedding metal by electroplating, sputtering, ion-implanting, or some other means, brazing with a metal filler can be accomplished as is normally done with metal substrates; that is, by simply selecting a filler that is compatible with the metalized surface material.

3.4.2.2 Noble Metal Brazing

Noble metal brazing is most commonly based with silver or platinum and their alloys, and somewhat less often based with copper or nickel, and occasionally based with other noble metals (e.g., palladium and gold) [58]. Such brazing is normally done in air, or even an oxygen-rich atmosphere, with evidence that noble metal oxides form and bond with the ceramic substrate, particularly with oxide ceramics. Correia et al. have thoroughly investigated the potential use of platinum as an interlayer (25 μm) between tetragonal zirconia polycrystal (TZP) and Ti-containing blocks within a wide temperature range [59]. Though the chemical reaction is strong, the interfaces are rather weak, actually failing at the interface between the TZP and the platinum-rich zone. In TZP/(Au-25 μm)/Ti joints brazed under vacuum, the infinite supply of Ti to the interface through the liquid Au results in a continuous interface without gaps. However, the Ti-Au intermetallics formed at the interface do not hinder Ti-diffusion toward the ceramic to form unfavorable Ti-oxides and Ti_xAu_y intermetallics [60]. Silver was also tested in the form of thin foil (35 μm) for the production of TZP/Ti joints at 980°C under vacuum. The interfacial reaction seemed stronger than in the Au case. A thick zone of a Ti-oxide (assigned to Ti_3O_2) formed at the interface featuring large holes. When zirconia was brazed to titanium and its alloys with palladium in an induction furnace, bonding formed at the interface. However, the brazed joint contains pores, thus the hermeticity of such joints is a problem.

3.4.3 Diffusion Bonding of Ceramic-to-Metal

Diffusion bonding eliminates any foreign material as needed in brazing so it would be preferred for implantable medical device applications. Alumina can be diffusion bonded to a few biocompatible metals including tungsten, platinum, molybdenum, stainless steel, and niobium [58, 61]. Zirconia has been successfully diffusion

bonded to niobium too. However, the poor machinability of niobium and molybdenum, and the poor mechanical properties of platinum have probably limited their applications. Zirconia-to-titanium alloy joints were also attempted by diffusion bonding [55, 59, 62] and low-strength joints were obtained, probably due to the Ti embrittlement caused by the enlargement of Ti-grains by two orders of magnitude. Diffusion bonding of TZP and Ti with a zirconium interlayer (30 μm) inserted between has been attempted by Agathopoulos et al. [62]; however, no successful joint has been reported.

3.5 Hermetic Seal with Fusion Welding

Fusion welding is often the final step in creating a hermetic seal for the implantable device. A variety of fusion welding methods used for hermetic metal-to-metal seals include laser-beam welding, electron-beam welding, resistance welding, and tungsten inert gas (TIG) welding, to name a few. The designers choose a particular welding method for their hermetic packages often based on the following considerations: the materials of the parts to be sealed, the specimen size, equipment availability, the joint configuration, and cost. Both laser-beam welding and electron-beam welding are high-energy welding processes. Laser-beam welding has become more and more popular over other methods in the recent years, most likely due to the following reasons:

1. Electron-beam welding requires a vacuum, while laser welding can be done in air or in an inert environment. Argon and helium mixtures are often the preferable inert laser-welding gas for protective purposes. Moreover, helium is the ideal gas for helium-leak testing.
2. Maintenance and operational costs for a laser-welding system are moderate.
3. A small heat-affected zone can be achieved with laser welding, which is particularly critical for the miniaturized implantable medical device, where too much heating or the close proximity of the heating zone might cause damage to the components inside the package.
4. No filler material is needed for laser welding with a properly designed weld joint.
5. Besides the challenge of designing a joint suitable for resistance welding, the process of hermetic sealing by resistance welding is often difficult, if it is even possible at all.

A successful laser weld in the application of a hermetic seal requires precision aiming stability, vibration isolation between the work surface and the environment, accurate location of the weld position, and real-time optical power feedback. Good coordination among the laser power supply, the motion control system, the vision system, the control computer, and operator is critical. Advanced laser-welding systems often have features, such as real-time power feedback, power ramping, and pulse shaping, to achieve the best weld quality possible.

Strong hermetic welds can be achieved by optimized laser parameters, proper joint design, and materials selection. Similar metallic materials are preferable for laser welding. Good welds can be obtained when welding titanium and its alloys, noble metals and their alloys, tantalum, and niobium. Welding Nitinol (a Nickel Titanium (NiTi) shape memory alloy composed of approximately 55% Nickel by weight) to itself has been successfully performed using laser welding [63], TIG welding, and resistance welding [64, 65]. 316 and 316 L stainless steels are considered among the most biocompatible of the stainless series, followed by 304 and 304 L stainless steels. A calculated Cr_{eq} to Ni_{eq} ratio of 1.52 to 1.9 is recommended to control the primary mode of solidification and prevent solidification cracks in type 304 L while the Cr_{eq}/Ni_{eq} ratio of 1.42 to 1.9 is recommended for type 316 L stainless steel [66]. Fusion welding of Tungsten tends to yield welds that are very brittle. Joining Nitinol to stainless steel is often difficult due to the formation of brittle intermetallic compounds such as FeTi and Fe_2Ti. Nitinol can be welded to other metals such as tantalum and niobium to yield acceptable joints [65]. Though joints with dissimilar metals can be achieved, issues such as galvanic corrosion have to be addressed when used in implantable medical device packages.

Frequently, more than one processing method can be used for assembling an implantable medical device. For example, ten critical joints of the first-generation neuromuscular microstimulator were accomplished by using four different technologies including infrared laser beam-assisted welding, TIG welding, resistance welding, and microsoldering [14]. Laser welding, active brazing, resistance welding, and microsoldering have been implemented for the second generation of neuromuscular microstimulators produced at The Alfred Mann Foundation, Santa Clarita, CA.

3.6 Conductive Vias on Ceramic Substrate

An alternative to the ceramic-to-metal feedthrough is the use of conductive vias on a ceramic substrate that can be produced by either high-temperature cofired ceramic (HTCC) or low-temperature cofired ceramic (LTCC). Because HTCC parts are fired at 1,400° to 1,500°C, refractory metals are often used for circuit traces, which results in high electrical resistance compared to noble metals. This resulting poor conductivity often has a detrimental effect on circuit performance. LTCC parts are fired at a lower temperature of about 950°C, so that silver and gold can be used as the conductor materials. Also, a wide variety of resistive and dielectric materials can be applied before firing to form passive components. Moreover, multiple layers with buried components can be formed, and active components with large I/O counts can be connected with wire bonding, surface mount, or flip chip techniques. These techniques allow unpackaged semiconductor device mounting, which further reduces board real estate for a given circuit configuration, so LTCC is often the preferred process. One application utilizing conductive vias on ceramic substrate is for the artificial retina where platinum-containing glass frit is used for the conductive vias

[67]. One challenge with utilizing the conductive vias on ceramic substrate parts for hermetic packaging is the limitation of high-temperature postprocessing of the ceramic substrate. In many cases, it is desirable to braze titanium and its alloys (for zirconia substrate) or niobium and its alloys or titanium-niobium (for alumina substrate) package walls to a via containing ceramic substrate to provide a means for achieving a final hermetic seal. It is possible that the hermeticity of the conductive vias could be compromised after the subsequent high-temperature processing.

4 Testing Methods for Hermetic Sealing of Implantable Medical Devices

4.1 Mechanical and Environmental Tests

An implantable active medical device should be constructed to not only withstand the mechanical forces that may occur during normal conditions of use, but also other possible environments – induced stresses, such as vibration, free fall; atmospheric pressure changes; and temperature changes during packaging, storage, transportation, and handling in an operating room. A list of mechanical tests often applicable to medical device packaging includes tensile, fatigue, vibration, shock, compression, and flexural testing. Environmental tests include temperature cycling, humidity, and corrosion tests. Refer to appropriate standards from the International Organization for Standardization (ISO), Association for the Advancement of Medical Instrumentation (AAMI), American Society for Testing and Materials (ASTM), and other agencies for detailed testing procedures.

The first-generation neuromuscular microstimulators consisted of a cylindrical glass capsule with a rigidly mounted electrode on each end, as shown in Fig. 4 [68]. It has been utilized for many applications from shoulder subluxation, to sleep apnea, to urinary incontinence, to foot drop, to knee osteoarthritis, to wrist and finger contractures, and to pressure ulcers [69, 70]. The mechanical integrity of the package has been tested by three-point bending over its long axis, tensile tests along its axial direction, free drop to steel instrument tray, five temperature cycles between autoclaving and freezing [14].

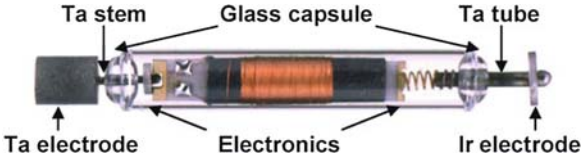

Fig. 4 The package of the first-generation neuromuscular microstimulator. (Reprinted from [71] with permission of Springer)

In 2006, Loeb et al. reported that among a total of 80 neuromuscular microstimulators that were implanted in 35 participants in five different clinical trials, four unresponsive implants were visibly broken as determined by X-ray analysis [71]. Two of the four failures occurred in adjacent neuromuscular microstimulators in

one patient after several months of tetanic stimulation to treat flexion contractures of the hand. Both had been inserted in the same orientation, with the Ta stimulation electrode located deep in the interosseous membrane to target nerves to the extensor muscles of the forearm. It is hypothesized that the failures of the clinical implants occurred as a result of repeated bending stress applied by the contracting muscle to the exposed 0.5-mm-long segment of the Ta stem, a ductile wire of 0.25 mm in diameter that is sealed into the relatively large glass capsule at one end and the Ta electrode at the other, as shown in Fig. 5. This was confirmed in a series of in vitro repetitive stress tests. Modifications were made to enhance the mechanical integrity of the glass package. This experience suggested the importance of appropriate mechanical tests to reveal the integrity of the device package prior to any application.

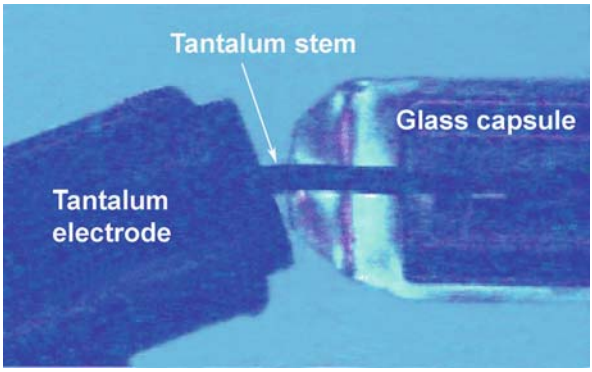

Fig. 5 A bent tantalum stem between the tantalum electrode and glass capsule. (Reprinted from [71] with permission of Springer)

4.2 Hermeticity Testing Methods and Their Limitations

High-quality hermetic seals place implantable medical devices among the most reliable assemblies [4]. Rigorous tests ensure the quality of the hermetic seals in such products. MIL-STD-883, Method 1014.10 provided details of the various hermeticity test procedures that have been adapted by the biomedical device industry. Generally speaking, a package with a standard air equivalent leak rate greater than 1×10^{-5} atm-cc/sec is considered a gross leaker. Packages with leakage below this rate are considered fine leakers. There are generally four methods of ascertaining a gross leak, including [41]:

1. Forcing a liquid, such as fluorocarbon liquid, into the package through the gross leak channel, vaporizing or decomposing this liquid in the package, thereby forcing the resultant gas out through the same leak channel, and then detecting the gas by the bubble test or the vapor detection test;

2. Forcing a liquid into the package, and then detecting its presence by a change in weight (the weight gain test) or by the deflection of the lid due to an increase in pressure by an interferometer;
3. Performing a dye penetrant test; and
4. Performing a residual gas analysis (RGA).

Helium-leak detectors, radioactive decay detectors, and interferometer (optical) leak detectors are all capable of fine leak detection. The most commonly used in the biomedical device industry is the helium-leak detector.

A helium-leak detector is a mass spectrometer tuned to analyze the helium gas. The detection limit of a helium-leak tester is generally 1×10^{-9} atm-cc/sec or better. Prior to the helium-leak test, the hermetic package is either subjected to high-pressure pure helium for a period of time ("bombed") or sealed in a helium-containing environment. Calibration of the helium-leak detector is presently accomplished using a calibrated helium-leak standard consisting of a small cylinder charged with helium at atmospheric pressure. The cylinder contains a filter through which helium exits at a fixed calibrated rate when the cylinder valve is opened, and the temperature at which the leak was calibrated is marked on the cylinder (typically 22–23°C). The calibrated helium-leak cylinder should be at this temperature when calibrating the system. Otherwise, an appropriate temperature compensation factor should be used in calculating the test object leak rate. When using the calibrated leak to set the sensitivity of the helium-leak detector, the detector meter is set for direct readout at the leak rate figure marked on the calibrated leak cylinder.

Radioactive decay is a technique in which a radioactive gas is placed inside the cavity of the device during device manufacture or by bombing after manufacture is complete. This technique is similar to the helium fine leak test method except that radioactive gas, such as krypton-85/dry N_2 mixture, is used. Krypton 85 is a radioactive inert noble gas that emits very weak gamma rays and beta particles. Parts are submerged in the radioactive gas for some time. After the part surfaces are free of residual radioactive gas, it is placed in a chamber connected to a scintillation crystal detection system that actually counts the number of Kr-85 particles inside the package. This is different from the helium fine leak test, which measures the rate of helium leaking out of the device. The leak rate of the device is calculated by a formula based on the concentration of Kr-85/N_2 tracer gas used, the bombing time and pressure, and the measured reading on the device. An Atomic Energy Commission license is necessary for possession and use of radioisotope test equipment and manufacturers are reluctant to use this method.

Optical leak testing is based on the deflection of the package lid when the pressure outside the package differs from that inside the package, either by evacuation or pressurization. The amount of deflection is measured by an interferometer, often a laser interferometer. Optical leak testing is not applicable to many devices where no suitable package configuration is available.

Fine and gross leak tests should be conducted in accordance with the requirements and procedures for the specific test conditions for the device. Combinations of fine and/or gross leak testing can be conducted in sequence or at the same time.

Cumulative Helium Leak Detection (CHLD) is a variation on conventional leak detection that allows for gross and fine leak testing in the same pass and the potential for helium-leak detection at leak rates several orders of magnitude lower than with conventional leak-detection methods.

For an implanted device with circuitry inside, moisture level is often considered the most critical piece of information as many electronic failures are directly related to moisture accumulation and condensation [36, 37, 40].

To some degree, the functional lifetime of a device can be estimated based on the moisture level accumulated inside the device. Lifetime estimation is commonly done with equation 1 based on when the moisture level inside the device reaches the dew point at body temperature, or the consensus [41] among scientists and engineers that the amount of liquid water necessary to promote corrosion is when three monolayers of liquid water form on the internal surface of the packaged device.

The dew point is a key parameter in controlling the ability of moisture condensation. The condensation process inside a package to form water droplets is a function of device temperature, internal pressure, and more importantly moisture level. With a known temperature and pressure, the dew-point level can be determined from the dew-point nomograph shown in Fig. 6 [72]. From the nomograph in Fig. 6, it can be seen that at 1.0 atm and 0°C, the moisture concentration needed for forming water droplets is 6,000 ppm. At levels below this percentage of water vapor, liquid drops will not be able to form. Hence, most materials and sealing processes are selected to keep the internal package environment at or below 5,000 ppm of moisture for the lifetime of the device. The rationale being that, at 5,000 ppm, the water vapor dew point is below the freezing mark, and therefore any moisture that would condense inside the package would be in the form of ice crystals and not be available for corrosion processes. Of course, one could argue that for implantable medical devices, the body temperature is about 37°C, so a higher moisture level should be allowed. But, some contaminants could promote moisture condensation considerably before the moisture reaches the saturation level of the dew point. A humidity test applicable to a specific medical device often has to be run to determine a safe moisture level as the baseline threshold.

$$t = -\frac{V}{L_{H2O}}\left[\ln\left(1 - \frac{Q_{H2O}}{\Delta pi_{H2O}}\right)\right] \tag{1}$$

Where: Q_{H2O} = the water that has leaked in the device in atm [41]

V = the available internal volume of the package (volume of the parts inside the package should be subtracted) in cc

t = the time in seconds

L_{H2O} = the true water leak rate = $0.471 * L_{\mathrm{He}}$ in atm-cc/sec

Δp_{iH2O} = the initial difference in the water partial pressure on the outside less the partial pressure on the inside the package (water vapor partial pressure in human body is 0.061 atm)

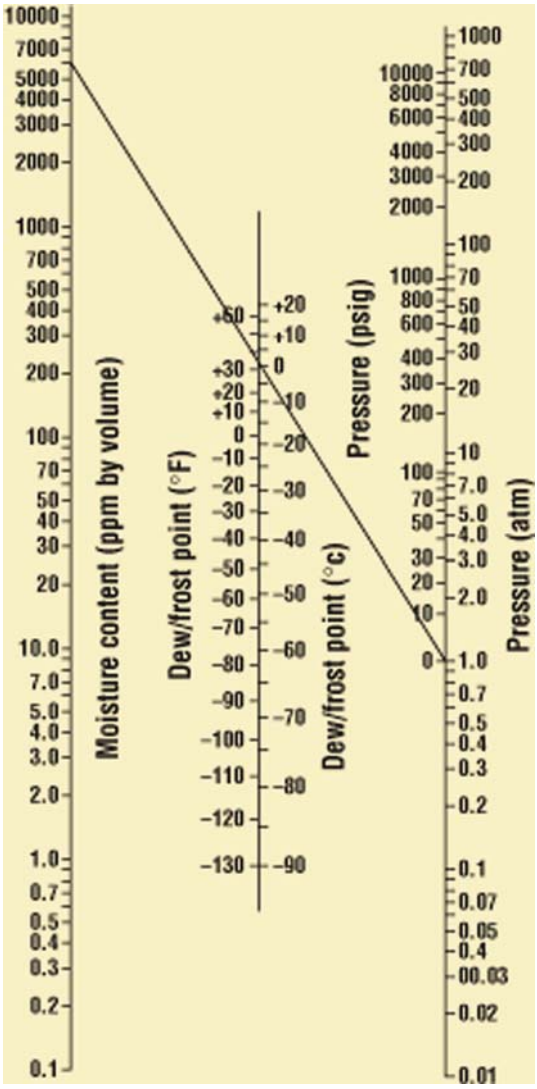

Fig. 6 Dew-point nomograph that correlates pressure, temperature, and water content (As shown, at 1.0 atm and 0°C, the dew point is 6,000 ppm of water). (Reprinted from [72] with permission of ASM International)

4.3 Biocompatibility Tests

The international standard organization ISO 10993 standard plays an important role in the assessment of the biocompatibility of a medical device. In principle, a great number of tests have to be undertaken depending on the intended use of the medical device. The standard describes tests on toxicity, carcinogenicity, and hemocompatibility, among others. Some of these tests are simple in vitro tests, while others require extensive animal experiments. For implanted medical devices,

where direct contact is made with blood, tissue, or bone (such as implantable cochlear implants), extensive in vitro and in vivo tests are required [73]. Refer to ISO 10993 for more discussion and detail on the selection of individual tests that should be done for a particular biological interaction or biological effect. In general, details of test methods are not given in the ISO documents and reference is made to other documents such as the American Society of Testing and Materials (ASTM) and The United States Pharmacopeia (USP) standards for procedures and methodologies. Most of the tests can be performed by laboratories specializing in biocompatibility testing. Listed below is the battery of tests often recommended by the FDA for Class III active implantable medical devices that make long-term contact with bone or tissue: cytotoxicity, sensitization, irritation or intracutaneous reactivity, acute systemic toxicity or pyrogenicity, subchronic toxicity, genotoxicity, implantation, chronic toxicity, and carcinogenicity. Additional tests, such as the hemo-compatibility testing, are required for blood contact implantable medical devices.

4.4 Corrosion Tests

Various electrochemical techniques have been employed to characterize the corrosion behavior of medical device packages [74]. Open-circuit potential measurements determine the corrosion potential of a metal in an electrolyte. Its value can be used to predict the long-term lifespan of metal packages under passive corrosion conditions. Corrosion rates and corrosion behavior of passive coating layers can be obtained by potentiodynamic or potentiostatic polarization methods, with which the polarization resistance and corrosion current density can be determined [75]. The breakdown potential, the potential above which surface pits are initiated, is usually defined as the potential at which there is a large increase in the response current. An anodic polarization curve measured on a Ti alloy is shown in Fig. 7. In the potential range of 0.3 to 1.1 V, a current plateau is visible, which indicates the Ti surface passivation. However, at higher potentials than 1.2 V, anodic current increases dramatically, suggesting surface activation or breakdown. When used as a metal case, care should be taken to make sure potential on the Ti surface does not exceed the breakdown potential.

Electrochemical Impedance Spectroscopy (EIS) is a powerful nondestructive method to characterize biomaterials. Electrode materials, solution resistance, electrode/electrolyte interface impedance, charge transfer resistance, and surface roughness/double layer capacitance can be measured and their frequency response properties can be determined in a fast frequency scan.

Cyclic voltammetry (CV) has been employed to determine the operational potential window (the water window) limited by the H_2 and O_2 evolution potentials due to electrolysis of water on the cyclic voltammogram.

There are several ASTM standards that describe electrochemical testing techniques for the evaluation of corrosion behaviors of metal materials. Two useful methods are ASTM G5 – 94: Standard Reference Test Method for Making

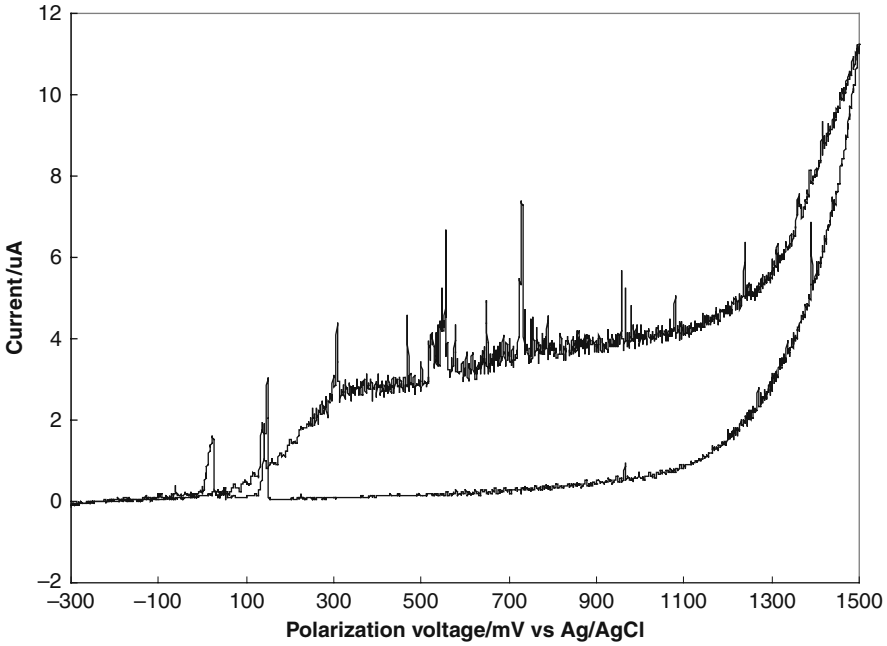

Fig. 7 An anodic polarization curve measured on a Ti alloy in saline solution at 37°C. The scan rate is 1 mV/second. See text for additional details

Potentiostatic and Potentiodynamic Anodic Polarization Measurements and ASTM G106 – 89: Standard Practice for Verification of Algorithm and Equipment for Electrochemical Impedance Measurements. Although most ASTM electrochemical testing techniques are developed for stainless steels, the test methods and procedures can be adapted for noble metals used in implantable medical devices.

Long-term stability of the metal package of medical devices is assessed in vitro through active soak tests under constant pulse stimulation. The packages are tested in buffered saline solutions at body temperature, or elevated temperatures for accelerated tests [76].

4.5 Morphological and Microstructural Characterization

Both light and scanning-electron microscopy (SEM) can provide valuable information about the surface of materials. The smoothness or roughness of surfaces can influence how materials interact with tissues and body fluids. Smoothness or roughness may also affect the binding of protein and biochemical intermediates (lymphokines and cytokines), which may also help determine a material's biocompatibility.

Electron microscopes create magnified images by using a beam of electrons as an imaging source. They resolve images at much higher magnifications than light microscopes can, often at magnifications up to 300,000 times. SEM can yield topographic images and elemental information when used in conjunction with energy-dispersive x-ray analysis (EDX) or wavelength-dispersive x-ray spectrometry (WDS). Elemental analysis using SEM/EDX or SEM/WDS is useful for qualitative and semiquantitative determination of elemental content and for obtaining correlation between microstructures and elemental composition.

Atomic force microscopy (AFM) is another powerful tool for examining the topography of a surface. It works much the same way as a profilometer does, only on a much smaller scale: a very sharp tip, often a silicon tip, is scanned across a sample surface at very short distance and the change in the vertical position reflects the topography of the surface. By collecting the amplified height data for a succession of lines it is possible to generate a three-dimensional map of the surface features with nanometer resolution. This instrument can also be used to evaluate crack formation and growth in both plastics and metals [77].

Other surface analytical techniques, such as x-ray photoelectron spectroscopy (XPS), Auger electron spectroscopy (AES) and secondary ion mass spectroscopy (SIMS) have been utilized to show that the elements of the titanium alloys are present in their surface oxides [78]. Transmission electron microscopy (TEM) and scanning transmission electron microscopy (STEM) studies showed that the oxides of the Ti-6A1-4 V alloy have a more complex microstructure and a different crystallinity, which are properties that could affect the biocompatibility of these titanium alloy implants.

X-ray diffraction enabled researchers to understand the microstructure of crystalline materials. To reveal the bonding mechanism of hermetic titanium alloys to yttria-stabilized tetragonal zirconia polycrystal (Y-TZP) ceramic-brazed joints, X-ray diffraction analysis on the fractured braze joints was conducted and revealed that the nickel titanium oxide (Ni_2Ti_4O) formed at the zirconia ceramic to titanium metal interface is responsible for the bonding [15].

4.6 Accelerated Life Test

For faster product development or improvement, accelerated life testing (ALT) can be used to determine the reliability of implants in accelerated use conditions [79]. Accelerated life testing helps to identify failures and failure modes qualitatively or predicts package lifetime quantitatively at normal use conditions (Accelerated Life Testing Online Reference, ReliaSoft's eTextbook for accelerated life testing data analysis [80]).

Among various stresses used to accelerate failures, temperature is widely accepted in accelerated life tests. The Arrhenius life-temperature model has been widely used in temperature-accelerated life testing [81]. The Arrhenius reaction rate equation proposed by the Swedish physical chemist Svante Arrhenius in 1887, is given by equation 2 [82]:

$$r = A \times \exp\left(-\frac{E_a}{kT}\right) \tag{2}$$

Where

r is the reaction rate
A is a constant with the unit $\sec^{-1}$ for first-order reactions
E_a is the activation energy (eV)
k is the Boltzman's constant (8.62×10^{-5} eV K^{-1})
T is the absolute temperature (Kelvin).

Practically, a modified equation derived from the above Arrhenius reaction rate equation is used to determine acceleration factors (K) in an accelerated life test for a package:

$$K = \exp\left[\frac{E_a}{k\left(\frac{1}{T_u} - \frac{1}{T_t}\right)}\right] \tag{3}$$

Where T_u is the intended use temperature of the device, i.e., body temperature in Kelvin and T_t is the elevated test temperature. It is clear from Eq 3 that the acceleration factor is sensitive to E_a at given test temperatures. The activation energy for the specific failure mode should be used in determining acceleration factors.

4.7 X-Ray Microscopy

X-ray microscopy permits nondestructive assessment of internal damage, defects, and degradation of a hermetic package. Illuminating a sample with X-ray energy provides images based on material density that allow for characterization of cracking, breakage, de-lamination, and defects in components. Figure 8 shows a void (about 75-μm wide) at the ceramic-to-metal joint interface of a brazed case package, which cannot be seen by visual inspection. X-ray microscopy has also been used as a 100% screening test for cochlear implants. However, cautions have to be

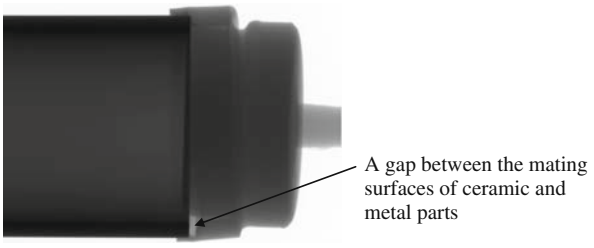

Fig. 8 A void at the ceramic-to-metal joint interface shown by X-ray imaging

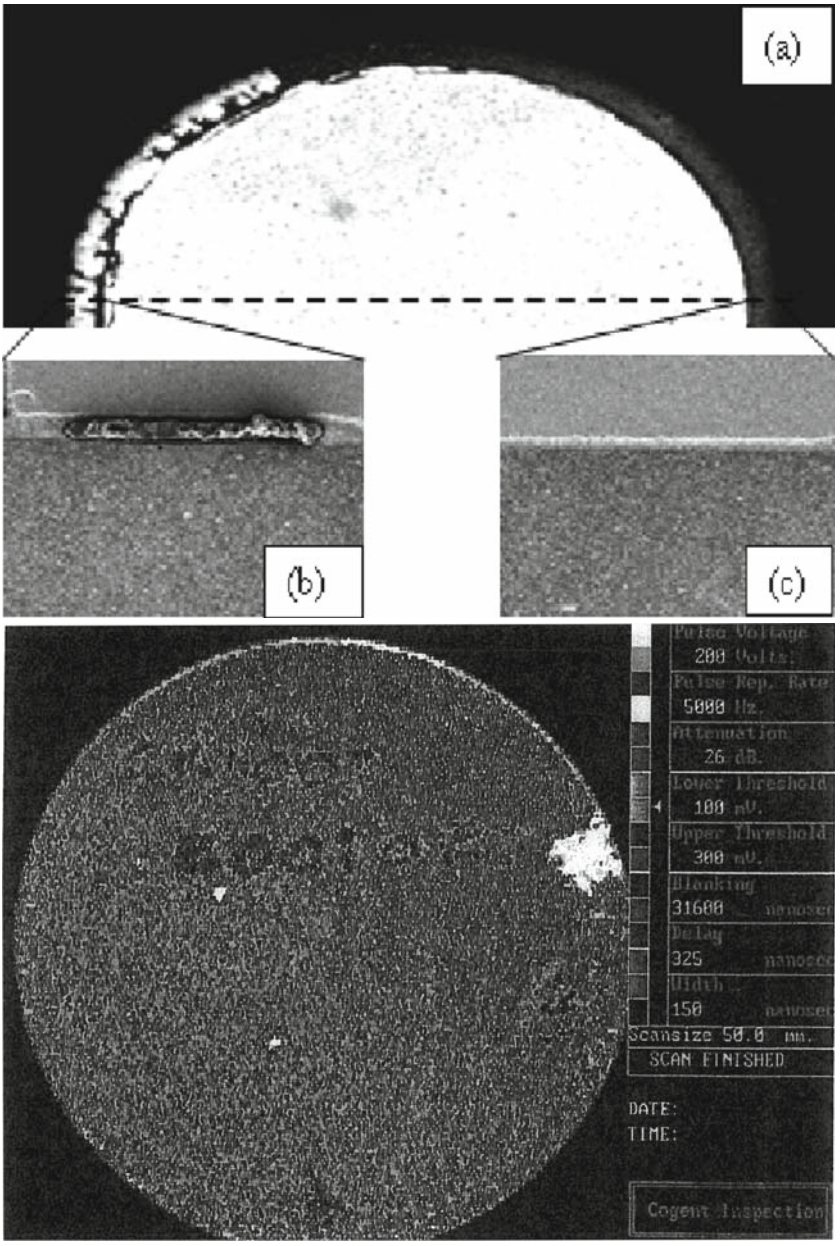

Fig. 9 SAM image (**a**) and SEM cross-section images corresponding to the left (**b**) and right (**c**) brazed areas in (**a**). Cross sectioning was done along the horizontal dotted line in (**a**). (**d**) SAM image of a 50-mm diameter brazed assembly showing a large edge-opening void at the right. (Reprinted from [83] with permission of ASM International)

taken when examining implantable medical devices containing memory chips, as an overdose of X-ray radiation can permanently erase the stored data and potentially cause device failure.

4.8 Acoustic Microscopy

Acoustic microscopy is another nondestructive testing method that uses acoustic impedance to produce high-resolution images of a sample's interior structure to detect "difficult-to-find" defects, such as interfacial separation in printed wiring boards, solder ball de-lamination in ball grid arrays, and die-attach voids, in processor element modules. Scanning acoustic microscopy (SAM) can be utilized for braze joint evaluation where the joint configuration is suitable [83]. Figure 9(a) is an SAM image of a brazed case. The large white oval area represents the body, and the gray ring on the right perimeter corresponds to a sound joint, while the white irregular area in the left perimeter corresponds to an area containing voids. Cross sectioning was made along the dotted lines and samples were prepared for SEM analysis. Figure 9(b) is the cross section of the white joint area in the SAM image where a huge void in the braze joint can be seen. Figure 9(c) is the cross section of the gray joint area in the SAM image where a good braze is shown. Figure 9(d) shows an SAM image of a 50-mm diameter assembly formed by vacuum brazing. Three voids are evident in the joint gap, including a large edge-opening void at the right [83]. For suitable joint configurations, SAM can be used for a 100% nondestructive screening test.

5 Challenges of Hermetic Packaging for Implantable Medical Devices

5.1 Long-Term Stability of Ceramic Materials

For many applications it is desirable that the implantable medical devices remain benign in the subject for the rest of the subject's life to avoid a secondary removal surgery. The intent is to leave the implanted neuromuscular microstimulator in the subject's body for the rest of his/her lifetime, which could be up to 80 or more years [15]. The cochlear implant is now the treatment of choice for children with profound and severe congenital and neonatal hearing loss [84, 85]. The long-term stability of the package for both of these devices is very important.

3 mole % Y-TZP (3Y-TZP) has much higher flexural strength and fracture toughness than the polycrystalline α–Al_2O_3. It has been adapted as the packaging material for both cochlear implants and neuromuscular microstimulators, because of an incident of fracture of an alumina-cased cochlear implant implanted in a young child. However, 3Y-TZP can suffer from low-temperature degradation (LTD) in moist environments. This aging phenomenon is caused by the transformation of

the crystalline structure from the tetragonal (T) phase to the monoclinic (M) phase, resulting in a decrease in strength and toughness, along with micro and macrocracking [86–88], which limits 3Y-TZP's long-term applications. Searching for new bioceramic materials that have improved antidegradation properties is currently one of the most active research fields. Alumina-toughened zirconia [89–91], zirconia-toughened alumina [92,93], Y-TZP with slight alumina doping [94], and zirconia ceramic with other oxide additions [95] all showed better hydrothermal stability than 3Y-TZP and have been proposed for potential use for long-term implantable packages. However, no report on their biocompatibility has been published and the manufacturing process of these materials is still maturing.

5.2 Metals and Alloys Corrosion

An implantable medical device is not only exposed to the harsh environment of the human body, but also to the electrical potential or current that is generated by the implantable medical device itself [7]. Corrosion is one of the major degradation mechanisms affecting the lifetime of metal packages used in medical implants in the body. The corrosion process will induce adverse biological reactions in the body and can lead to mechanical failure of the implants. The packaging materials or construction must eliminate the corrosion risk in the body in both passive and active conditions.

The driving force for passive electrochemical corrosion in a biological environment is the potential variation between the different materials. A typical example of passive corrosion processes is galvanic corrosion. When two dissimilar metals are in contact with each other and exposed to an electrolyte, a potential is set up between the two metals and a galvanic couple is formed. In the presence of an electrolyte, this galvanic couple acts as an electrochemical corrosion cell. In this galvanic couple, one less noble metal will become the anode while the more noble material will act as the cathode in the corrosion cell. The potential difference will result in electrochemical reactions and generate current flow in the corrosion cell, and the oxidation reaction in the cell will cause the anode to corrode. Moreover, the corrosion rate for the metals will be altered when they form a galvanic couple, and the corrosion of anodic material in the corrosion cell will be accelerated by the cathode and subsequently will corrode faster than it would have all by itself.

Crevice corrosion is another passive corrosion process which will cause localized corrosive attack. Crevice corrosion may occur in small occluded areas of a stagnant solution or in crevices where the metals are shielded from full exposure to the surrounding environment. The occluded portion of metal surface has a lower oxygen concentration than the surrounding medium due to restricted oxygen diffusion into the shielded areas. Such localized oxygen concentration difference in crevices will form a potential difference and initiate galvanic corrosion on the anode. In the crevice corrosion cell, the lower oxygen portion in the crevice acts as an anode while the exposed portion with higher oxygen acts as a cathode.

Active electrochemical corrosion on a metal package is driven by the potential or current, which is generated during neural stimulation by an implant. Most neurostimulation applications use a charge-balanced, biphasic, cathodic-first current pulse. When the metal package of an implantable device is used as a return electrode, active electrochemical corrosion will cause metal dissolution. Depending on the current density or charge density applied, the resulting voltage on the metal package may exceed the safe electrochemical window to induce irreversible Faradaic reactions, including anodic dissolution and oxide formation. In an extreme condition, the electrode voltage on the metal package may exceed water window potentials to cause water electrolysis and gas evolution. Hydrogen or oxygen evolution due to water electrolysis that is induced by a stimulus will alter pH [96]. Oxygen evolution during anodic phase will decrease pH, while hydrogen evolution in cathodic phase will increase pH. Such changes in pH will cause metal corrosion and possible tissue damage in the electrode/tissue interface [97]. High pH produced by the cathodic reaction of water analysis reduction leads to dissolution of the passive oxidation layer. A recent study on hydrogen gas evolution induced by neural stimulus revealed that free chlorine (in the forms of HOCl, ClO^-, and Cl_2) was also detected along with the hydrogen evolution [98]. It appeared that the hydrogen and chlorine evolution reactions proceeded simultaneously at rates directly related to the charge injected.

Alloys used in the brazing process of the metal package are susceptible to dealloying corrosion. In a dealloying corrosion process, one or more elements are selectively dissolved, leaving behind a porous residue of the remaining elements [99]. Under a high stimulus, the resulting electrode voltage may exceed a critical potential that indicates the transition from passive and stable alloy to rapid dealloying. Dealloying of metal packages will lead to stress corrosion cracking and will eventually compromise hermeticity.

5.3 Challenges in Accelerated Life Test

Accelerated life tests usually take too long to be conducted online, as part of any product development cycle. Therefore, they must be conducted offline, well before the components, materials, or processes are needed for a given application. For these reasons, ALT is usually conducted generically, using generic samples which represent the materials, components, and processes used for a variety of products [100].

The most significant potential problem with quantifiable accelerated testing is that failure modes produced might not be modes occurring under normal operating conditions [101]. Thus care should be taken in an accelerated life test to keep failure modes unchanged from a normal use condition. Often, multiple failure modes are associated with packages under tests. In order to achieve a reliable lifetime prediction, the acceleration conditions and the accelerated factors should be identified for each failure mechanism. In the case of the ceramic-to-metal package for the second-generation microstimulator, there are two possible failure modes: one mode is the

loss of the hermeticity of the package due to corrosion occurred in the ceramic-to-metal seal. The second is 3Y-TZP ceramic surface flaking or self-transformation. The second mode is more likely when a qualified ceramic-to-metal joint is provided. A reliable lifetime prediction of the microstimulator package has been done by determining the Arrhenius factor of the ceramic degradation based on quantitative information obtained from an accelerated aging test with a dummy microstimulator ceramic-to-metal package at a series of temperatures and in vivo studies carried out with microstimulator implants in sheep and rats [15]. It is concluded that a neuromuscular microstimulator packaged with 3Y-TZP ceramic can remain hermetic and retain the ability to withstand a minimum of 15 pounds of cracking load in three-point bending tests after what is equivalent to 70 years of implantation in a human body.

To ensure the acceleration test conditions and factors truly correlate the failure modes produced by ALT with those that occur in normal use conditions, real-time tests should be carried out in parallel with the accelerated tests [102].

5.4 Hermeticity Test Reliability for Miniature Devices

Miniaturization of implantable medical devices continuously poses challenges to hermetic packaging practices. For example, the reliability of hermetic tests decreases with the further reduction of device size. Assuming no moisture is present within a sealed package at the final seal, and no moisture outgassing from the internal material after final sealing, at 1×10^{-10} atm-cc/sec helium-leak rate (4.71×10^{-11} atm-cc/sec moisture leak rate), a calculation based on equation 1 suggests that it will take less than 2 years to reach the 5,000 ppm moisture level in a 0.05 cc package. To guarantee a 10-year functional life (based on a final moisture level $\leq$5,000 ppm) of a medical device with a smaller internal free volume of 0.005 cc, a true helium-leak rate of 6.05×10^{-15} atm-cc/sec (an equivalent H_2O leak rate of 2.85×10^{-15} atm-cc/sec) is required. This is certainly beyond the capacity of any helium-leak detector currently available. The current state-of-the-art for helium-leak testing is claimed by a manufacturer that states that its cumulative helium-leak detector has a 1×10^{-13} atm-cc/sec true helium-leak rate capability [103]. This equipment utilizes metallic seals to eliminate any polymer/plastic seals that could absorb helium. The real operational leak-rate detection capability is about 5×10^{-12} atm-cc/sec and the productivity is limited. A separate room with good ventilation is needed to maintain a low-helium background level for this equipment, and a single use metal o-ring is required for each part to be tested.

The requirement of a helium-leak test for a MEMS device package with an internal volume of around 0.001 cc or below for chronic implantation (>10 years) is definitely beyond the capability of any current helium-leak detector. That is where getter materials come into play. A getter material can absorb various gaseous species and can be used to extend the effective lifetime of a medical device by absorbing moisture and other detrimental gas species, such as hydrogen [104–106] and oxygen [40].

5.5 Design challenges for Miniature Devices

The reduced size of implantable medical devices means the amount of water necessary to increase the humidity to corrosive levels in the interfacial environment becomes exceedingly small. It takes a shorter period of time for moisture or other ions to go through a narrower sealing wall or an interfacial pathway. Higher quality bulk materials and void-free interfacial sealing are essential to achieve the same degree of reliability for a smaller package than a bigger one. The challenges associated with hermetic seal design and material processing also increase with further reduction in device size [107].

5.6 Hermetic Packaging of MEMS for Implantable Medical Devices

There is tremendous interest in the development of MEMS for medical applications. In the most general sense, MEMS refers to miniature components or systems that are fabricated using techniques that were originally developed by the microelectronics fabrication industry, and then modified for the production of microstructures, micromachines, or microsystems such as sensors and actuators [108–110]. Currently, there are numerous research, development, and commercialization efforts underway to create high-performance clinical devices by exploiting the potential for size miniaturization and integration with microelectronics afforded by microfabrication and micromachining techniques [108, 111–114].

Materials commonly used in the fabrication and packaging of standard MEMS devices, including silicon, silicon dioxide, silicon nitride, polycrystalline silicon, silicon carbide, titanium, and SU-8 epoxy photoresist, were evaluated for cytotoxicity using the ISO 10993-5 standard [115, 116]. The data from this evaluation indicated that all above-mentioned MEMS materials are suitable candidates for the development of implantable medical devices. The deployment of implantable MEMS devices based on the silicon and related microelectronics materials has generally relied on protective coatings, such as biocompatible silicone gels, to isolate the MEMS components from the hostile body environment. Two primary drawbacks can result from this protective packaging approach: attenuation of signal/stimulus that must be communicated between the physiological environment and the device and an increased size that detracts from the benefits of miniaturization particularly when working in constrained spaces or at the cellular level.

Several hermetic packaging technologies could potentially lead to successful deployment of MEMS for implantable medical devices [107–111]:

Najafi et al. have developed a biocompatible hermetic package with high-density multifeedthroughs designed to withstand corrosive environments [107, 108]. This technology utilizes electrostatic bonding of a custom-made glass capsule to a silicon substrate to form a hermetically sealed cavity. Even though biocompatibility and long-term stability have been demonstrated, the required high voltage (2,000 V) and high temperature (320 to 350°C) during the process limits its applications.

"Epi-seal" encapsulation developed by Kenny et al. at Stanford University consists of a 20∼50-μm thick epitaxially grown polysilicon encapsulation layer covered by 4 μm passivation oxide. Aluminum partially covers the encapsulation to form electrical interconnects [109]. Investigation on the hermeticity and diffusion behaviors of "epi-seal" wafer-scale polysilicon thin-film encapsulation revealed that hermeticity of the encapsulation is gas species specific: hydrogen and helium easily travel in and out of the encapsulation, but nitrogen and argon do not [110].

Chiao and Lin reported that a glass-silicon package formed by rapid thermal processing aluminum-to-silicon nitride bonding can be used for MEMS packaging applications; a Pyrex® (Corning 7740) glass is used [111]. Accelerated hermeticity testing showed that for packages with a sealing ring width of 200 μm and an average sealing area of 1,000 × 1,000 μm^2, the lower bound of the 90% confidence interval of mean time to failure is estimated as 270 years under "tropical" conditions (35°C, 1 atmosphere and 95% relative humidity).

6 Conclusions

Advances in hermetic packaging technology have helped in the successful commercialization of many implantable medical devices, including implantable pacemakers, cardioverter defibrillators, implantable neuromuscular stimulators, and cochlear implants. The continued success of such devices is very much dependent on the reliability of the hermetic package. The packaging methods discussed in this chapter will continue to play important roles in the realm of hermetic packaging for implantable medical devices.

Many issues associated with hermetic packaging have yet to be completely understood, let alone overcome. The continued miniaturization of future implantable medical devices provides both opportunities and challenges for packaging/materials engineers to improve the current packaging methods and to develop new methods. Reliable hermetic micropackaging technologies are the key to a wide utilization of MEMS in miniaturized implantable medical devices.

Acknowledgements The authors would like to thank the Alfred Mann Foundation and Second Sight Medical Product Inc. for their support while they were working on this manuscript. They also thank Dr. Schnittgrund G, Dr. Duttaahmed S, and Grannis S for their detailed review of the manuscript.

References

1. FDA Consumer (2000) 34(2):7
2. Thwaites T (1995) Total recall for medical implants: New Scientist, p. 1212
3. Tummala R, Rymaszewski E (1989) Microelectronics packaging handbook, New York, Van Nostrand Reinhold
4. Ely K (2000) Manufacturing issues in hermetic sealing of medical products, http://www.devicelink.com/mddi/archive/00/01/015.html. Accessed 20 Jan 2008
5. Bhadra N, Kilgore KL and Peckham PH (2001) Implanted stimulators for restoration of function in spinal cord injury, Medical Engineering and Physics. 23:19–28

6. Strojnik P, Peckham PH (2006) Implantable stimulators for neuromuscular control. In: Bronzino JD (ed) Medical devices and systems, The biomedical engineering handbook, 3rd edn. CRC Press, Taylor and Francis Group, Boca Raton, FL
7. Nichols M F (1994) The challenges for hermetic encapsulation of implanted devices- A review, Biomed. Eng. 22(1): 39–67
8. Lussignea RW (1997) Liquid crystal polymers: new barrier materials for packaging, Packaging Technology, October 1997
9. Farrell B, Jaynes P, Johnson W et al. (2003) The liquid crystal polymer packaging solution, Proc. IMAPS 2003 International Symposium, Boston, MA pp 18–23
10. Loeb GE, Byers CL, Rebscher SJ et al. (1983) Design and fabrication of an experimental cochlear prosthesis. Med & Biol Eng Comput, 21:241–254
11. Forde M, Ridgely P (2006) Implantable cardiac pacemakers. In: Bronzino JD (ed) Medical Devices and Systems, The Biomed Eng handbook, 3rd edn. CRC Press, Taylor and Francis Group, Boca Raton, FL
12. Duffin EG (2006) Implantable defibrillator. In: Bronzino JD (ed) Medical Devices and Systems, The Biomed Eng handbook, 3rd edn. CRC Press, Taylor and Francis Group, Boca Raton, FL
13. McDermott H (1989) An advanced multiple channel cochlear implant. Biomedical Engineering, IEEE Transactions on. 36:789–797
14. Loeb GE, Richmond FJR (2001) BION^{TM} implants for therapeutic and functional electrical stimulation. In: Chapin JK, Moxon KA (ed) Neural prostheses for restoration of sensory and motor function. CRC Press, Boca Raton, FL
15. Jiang G (2005) Development of ceramic-to-metal package for BION microstimulator, Ph.D. dissertation, University of Southern California
16. Hochmair I, Nopp P, Jolly C et al. (2006) Trends in Amplification, 10 (4):201–220
17. Weiland JD, Liu W, Humayun MS (2005) Retinal Prosthesis, Annu. Rev. Biomed. Eng. 7:361–401
18. McKinney JRV, Lemons J (1987) The dental implant, PSG Publ., Littleton, MA
19. Hulbert SF, Bokros JC, Hench LL et al. (1987) Ceramics in clinical applications: Past, present, and future, in High Tech Ceramics, Vincenzini P ed, Elsevier, Amsterdam, pp189–213
20. Christel P, Meunier A, Dorlot JM et al. (1988) Biomechanical compatibility and design of ceramic implants for orthopedic surgery, in Bioceramics: materials characteristics versus in-vivo behavior. Ducheyne P and Lemons J, eds. Ann New York Acad Sci 523:234
21. Hulbert S (1993) The use of alumina and zirconia in surgical implants. In: An introduction to bioceramics. Hench LL and Wilson J, eds. World Scientific, Singapore, P25–40
22. Miller JA, Talton JD, Bhatia S (1996) in Clinical performance of skeletal prostheses, Hench LL, Wilson J eds, Chapman and hall, London, p41–56
23. Piconi C, Maccauro G (1999) Review: zirconia as a ceramic biomaterial. Biomatls 20:1–25
24. Tsukuma K, Shimada M (1985) Strength, fracture toughness and vickers hardness of CeO_2-stabilized tetragonal ZrO_2 polycrystals (Ce-TZP). J of Matls Sci 20:1178–1184
25. Schneider SJ (ed) (1991) Ceramics and glasses In: Engineered Materials Handbook, Volume 4, ASM International
26. Schwartz MM (1992) Handbook of structural ceramics, McGraw-Hill Publishers, USA
27. Guillou MO, Henshall JL, Hooper RM et al. (1992) Indentation fracture testing and analysis, and its application to zirconia, silicon carbide and silicon nitride ceramics. J of Hard Matls 3:421–434
28. Whitney ED (1994) Ceramic cutting tools – materials, development and performance, Noyes Publications, Park Ridge, NJ
29. Griffin EA, Mumm DR, Marshall DB (1996) Rapid prototyping of functional ceramic composites. Amer Ceram Soc Bull 75:65–68
30. Jiang G, Mishler D, Davis R et al. (2005) Zirconia to Ti-6Al-4 V braze joint for implantable biomedical device. J of Biomed Mater Res: Part B – Applied Biomatls 72B:316–321

31. Daulton J (2006) Self-centering braze assembly, US patent: 7,132,173 B2
32. Haller MI, He TX, Daulton J (2006) Electrode assembly for a microstimulator, US patent: 7,103,408 B2
33. Loeb GE, Richmond FJR, Baker LL (2006) The BION devices: injectable interfaces with peripheral nerves and muscles, Neurosurg Focus 20 (5):E2
34. Webster JG (1978) Medical instrumentation application and design, Houghton Mifflin, Boston
35. Williams DF (1981) Biocompatibility of clinical implant materials, Vols 1 and 2, CRC press, Boca Raton, FL
36. Thomas RW (1976) Moisture, myths, and microcircuits, in IEEE Trans. On Parts, Hybrids, and Packaging, p167–171
37. DerMarderosian A (1978) Electrochemical migration of metals, Proc. Int'l Microelectronics Symp., pp134–141
38. Grunthaner FJ, Griswold TW, Clendening PJ (1975) Migratory gold resistive shorts: chemical aspects of a failure mechanism, Proc. 13th annual proceedings. International reliability physics symposium, pp 99–106
39. DerMarderosian A, Murphy C (1977) Humidity threshold variations for dendritic growth on hybrid substrate, Proc Int Reliability Phys Symp, Las Vegas, NV
40. Roswell AE, Clymer GK (1971) Thermal fatigue lead-soldered semiconductor device, US Patent 3,735,208
41. Greenhouse H (1999) Hermeticity of electronic packages, Noyes Publication / William Andrew Publishing LLC, Norwich, New York, USA
42. Wong CP (1998) Polymers for encapsulation: materials processes and reliability, Chip scale review, Vol. 2, No. 1, 30
43. Donaldson PEK (1983) The cooper cable: an implantable multiconductor cable for neurological prostheses. J of medical and biological engineering and computing 21:371–374
44. Lovely DF, Olive MB, Scott RN (1986) Epoxy moulding system for the encapsulation of microelectronic devices suitable for implantation, J. of medical and biological engineering and computing, Vol24, No. 2:206–208
45. Loeb GE, Bak MJ, Salcman M et al. (1977) Parylene as a chronically stable, reproducible microelectrode insulator, IEEE Trans. Biomed. Eng., 24 (2):121–128
46. Yuen TG, Agnew WF, Bullara LA (1987) Tissue response to potential neuro-prosthetic material implanted subdurally. Biomaterials, 8 (2):138–141
47. Stieglitz T (2005) Methods to determine the stability of polymer encapsulations. The 10th annual conference of the international functional electrical stimulation society, Montréal, Canada
48. Donaldson PEK (1976) The encapsulation of microelectronic devices for long service life. IEEE trans. Biomed. Eng., 23:281–285
49. Petersen ME, Sergent J (1979) Metal hermetic package selection, Electronic Packaging and Production, p. 150–156
50. Graeme C (2003) Cochlear implants, fundamentals and applications, AIP series in modern acoustics and signal processing by Beyer RT (editor in chief) Springer, New York
51. Bealka JD, Da Costa PH (2003) Feedthrough devices, US patent: 6,586,675 B1
52. Mastrogiacomo J (2007) New ceramic technology contributes to advances in medical implants, http://www.morgantechnicalceramics.com/articles/medical_implants.htm. Accessed 20 Jan 2008
53. Peytour C, Berthet P, Barbier F et al. (1990) Interface microstructure and mechanical behavior of brazed Ti6Al4V/zirconia joints, J. Mater. Sci. Lett, 9:1129–31
54. Santella ML, Pak JJ (1993) Brazing titanium-vapor-coated zirconia. Welding Res Supplement, 165–172
55. Agathopoulos S, Moretto P, Peteves SD et al. (1997) Brazing of zirconia to Ti and Ti6Al4V. In 1996 Amer Ceram. Soc. Meeting, Indianapolis, USA 1996, Ceram Joining, Ceram Trans. Indianapolis 77:75–82

56. Lasater BJ (2001) Methods for hermetically sealing ceramic to metallic surfaces and assemblies incorporating such seal, US Patent: 6,221,513 B1
57. Fey K and Jiang G (2003) Application and manufacturing method for a ceramic to metal seal; US Patent: 6,521,350 B2
58. Messler RW (2004) Joining of materials and structures-–from pragmatic process to enabling technology, Elsevier Butterworth Heinemann, Burlington, MA
59. Correia RN, Emiliano JV, Moretto P (1998) Microstructure of diffusional zirconia-titanium and zirconia-Ti6Al4V alloy joints. J Matl Sci 33:215–221
60. Agathopoulos S, Correia RN, Joanni E et al. (2002) Interactions at zirconia-Au-Ti interfaces at high temperatures, Key Eng Matls 206–213:487–90.
61. Messler RW (1993) Joining of advanced materials, Elsevier Butterworth Heinemann Science, Burlington, MA
62. Agathopoulos S, Pina S, Correia RN (2002) A review of recent investigations on zirconia joining for biomedical applications. Ceram Trans 138:35–147
63. Falvo A, Furgiuele FM, Maletta C (2005) Laser welding of a NiTi alloy: Mechanical and shape memory behavior. Materials Science and Engineering: A. 412:235–240
64. Wu MH (2001) Fabrication of Nitinol materials and components, Proceedings of the international conference on shape memory and super-elastic technologies, Kunming, China, 285–292
65. Schetky LM, Wu MH (2003) Issues in the further development of Nitinol properties and processing for medical device applications, Proceedings from the Materials & Processes for Medical Devices Conference, Anaheim, California, pp 271–276
66. Korinko PS, Malene SH (2001) Considerations for the weldability of types 304 L and 316 L stainless steel. J of failure analysis and prevention 1:61–68.
67. Greenberg RJ, Mann AE, Talbot N et al. (2007) Biocompatible bonding method and electronics package suitable for implantation, US Patent: 7,211,103
68. Loeb GE, Zamin CJ, Schulman JH et al. (1991) Injectable microstimulator for functional electrical stimulation, North Sea Conference on Biomedical Engineering, Antwerp, Belgium
69. Singh J, Peck RA, Loeb GE (2001) Development of BION Technology for functional electrical stimulation: Hermetic Packaging, Proc. IEEE-EMBS Istanbul, Turkey
70. Dupont AC, Bagg SD, Chun S et al. (2002) Clinical Trials of BION^{TM} Microstimulators, Proc. IFESS, Ljubljana, Slovenia
71. Loeb GE, Peck RA, Singh J et al. (2006) Mechanical loading of rigid intramuscular implants, Biomed microdevices, Vol . 9, No. 6:901–910
72. ASM International (1989) Electronic material handbook, Packaging Vol. 1, CRC press
73. Ligtvoet KM, Wijcherson A, Bakker EJ (2005) Biocompatibility of medical devices, In: DI Sens symposium-book
74. Mansfeld F (2003) The use of electrochemical techniques for the investigation and monitoring of microbiologically influenced corrosion and its inhibition – a review. Materials and Corrosion 54:489–502
75. Chohayeb AA, Fraker AC, Eichmiller FC et al. (1996) Corrosion Behavior of Dental Casting Alloys Coupled with Titanium, in Medical Applications of Titanium and Its Alloys: The Material and Biological Issues, ASTM STP 1272, S. A. Brown and J. E. Lemons, eds., American Society for Testing and Materials, West Conshohocken, PA
76. Zhou D, Mech B, Greenberg R (2000) Accelerated corrosion tests on Silicon wafers for implantable medical devices. Proc., of 198th Electrochemical Society Meeting, p363
77. Goken M (1999) Atomic Force Microscopy of Metallic Surfaces. Adv Matls & Processes 155:35–37
78. Lausmaa J, Ask M, Rolander U et al. (1989) Preparation and analysis of Ti and alloyed Ti surfaces used in the evaluation of biological response. Mater. Res. Soc. Symp. Proc. 110:647–653

79. Meeker and Hahn (1985) How to plan an accelerated life test: some practical guidelines, The ASQC basic references in quality control, Vol. 10
80. http://www.weibull.com/acceltestwebcontents.htm, accessed on 10 March, 2008.
81. Nelson W (1990) Accelerated testing, statistical models, test plans, and data analysis, John Wiley & Sons, New York
82. Parker SP (editor-in-chief) (1994) McGraw-Hill Dictionary of Scientific and technical Terms, 5th edition, McGraw-Hill
83. Jacobson DM, Humpston G (2005) Principles of brazing, ASM International, p165.
84. Osberger MJ (1997) Current issues in cochlear implants in children. The hearing review, Vol 4, p 29
85. Severens JL, Brokx JPL and van den Broek (1997) Cost analysis of cochlear implants in deaf children in the Netherlands. Amer J of Otology 18:714
86. Tsukuma K, Kubota Y, Tsukidate T (1984) Advances in ceramics, Vol. 12, Science and technology of zirconia II. Edited by N. Claussen, M. Ruhle, and A. H. Heuer. American Ceramic Society, Columbus, OH, p. 382
87. Sato T, Shimada M (1985) Transformation of Yttria-doped Tetragonal ZrO_2 Polycrystals by Annealing in Water. J Am Cer Soc 68 (6): 356–369
88. Somiya S, Yoshimura M (1987) Zirconia ceramics, Uchida Rokakuho Publishing Co., Ltd, Tokyo
89. Li JF and Watanabe R (1999) Mechanical properties of PSZ-matrix ceramic composites containing Al2O3 particles with various sizes. Key Eng Matls 161–163:299–302
90. Begand S, Oberbach T, Glien W (2005) ATZ – a new material with a high potential in joint replacement. Key Eng Matls 284–286:983–986
91. Begand S, Oberbach T, Glien W et al. (2008) Kinetic of the phase transformation of ATZ compared to biograde Y-TZP. Key Eng Matls 361–336:763–766
92. Ikeda1 J, Pezzotti G, Nakanishi T (2006) Phase stability of zirconia toughened alumina composite for artificial joints. Key Eng Matls 309–311:1243–1246
93. Begand S, Oberbach T, Glien W (2007) Corrosion behavior of ATZ and ZTA ceramics. Key Eng Matls 330–332:1227–1230
94. Zhang B, Isobe T, Satani S et al. (1999), The effect of alumina addition on phase transformation and mechanical properties in partial stabilized zirconia. Key Eng Matls 161–163:307–310
95. Hirano M, Inada H (1991) Hydrothermal stability of yttria- and ceria-doped tetragonal zirconia-alumina composites. J of Matls Sci 26:5047–5052
96. Zhou D, Chu A, Agazaryan A et al. (2004) Towards an implantable micro pH electrode array for visual prostheses, in Nanoscale Devices, Materials, and Biological Systems: Fundamentals and Applications (Cahay M ed.) pp. 563–576. Electrochemical Society
97. Huang CQ, Carter PM, Shepherd RK (2001) Stimulus induced pH changes in cochlear implants: An *in vitro* and *in vivo* Study. Annals of Biomedical Engineering 29:791–802
98. Sanders C, Nagler E, Zhou D et al. (2007) Dynamic Interactions of Retinal Prosthesis Electrodes with Neural Tissue and Materials Science in Electrode Design, in Artificial Sight, Basic Research, Biomedical Engineering, and Clinical Advances, Humayun MS et al. (Eds.) Ch 11:209–226, Springer
99. Dursun A, Pugh DV, Corcoran SG (2003) A Steady-State Method for Determining the Dealloying Critical Potential. Electrochemical and Solid-State Letters, 6 (8) B32–B34
100. http://www.tutorialsweb.com/reliability/reliability4.htm#r4.1, accessed on 10 March, 2008.
101. Utter RE (2005) Accelerated life test – your key to new product success. http://www.innovativethermal.com/articles/, accessed 10 March, 2008
102. Edell DJ (2004) Insulating biomaterials in Neuroprosthetics, Theory and Practice, edited by Horch KW & Dhillon GS, pp. 517–579

103. Pernicka JC (2006) Pernicka unveils world's first CHLD hermeticity test system for medical and space applications, available online at http://www.pernicka.com/Press_CHLD.htm, Accessed 10 March, 2008
104. Bredendiek-Kämper S, Klewe-Nebenius H, Pfennig G et al. (1989) Surface analytical characterization of the hydrogen getter material ZrCo. Fresenius' Journal of Analytical Chemistry 335:669–674
105. Lee SM, Park YJ, Lee HY et al. (2000) Hydrogen absorption properties of a Zr–Al alloy ball-milled with Ni powder, Intermetallics 8:781–784
106. Liu CZ, Shi LQ, Xu SL et al. (2004) Kinetics of hydrogen uptake for getter materials. Vacuum 75:71–78
107. Ramesham R, Ghaffarian R (2000) Challenges in interconnection and packaging of microelectromechanical systems (MEMS) Electronic Components and Technology Conference Proceedings. 50th Volume , Issue 2000:666–675
108. Roy S, Ferrara LA, Fleischman AJ et al. (2001) Micro-electromechanical systems and neurosurgery: a new era in millennium. Neurosurgery 49:779–797
109. Roy S, Fleischman AJ (2003) Cytotoxicity evaluation for microsystems materials using human cells. Sens and Mat., 15:335–340
110. Roy S, Mehregany M (1999) Introduction to MEMS. In Helbajian H (ed.), Microengineering aerospace systems. The aerospace press, El Segundo, CA pp 1–28
111. Ferrara LA, Fleischman AJ, Togawa D et al. (2003) An in vivo biocompatibility assessment of MEMS materials for spinal fusion monitoring. Biomed Microdev 5:297–302
112. Fleischman AJ (2003) Miniature high frequency focused ultrasonic transducers for minimally invasive imaging procedures. Sens Actu A: Phys 103:76–82
113. McAllister DV, Allen MG, Prausnitz MR (2000) Micro-fabricated micro-needles for gene and drug delivery. Ann Rev Biomed Eng 2:289–313
114. Polla DL, Erdman AG, Robbins WP et al. (2000) Microdevices in medicine. Ann Rev Biomed Eng, 2:551–576
115. Kotzar G, Freas M, Abel P et al. (2002) Evaluation of MEMS materials of construction for implantable medical devices. Biomaterials 23:2737–2750
116. Roy S, Ferrara LA, Fleischman AJ et al. (2007) MEMS and neurosurgery, In Ferrari M (editor in chief) BioMEMS and biomedical nanotechnology, Vol 3: Therapeutic Micro/nanotechnology (ed. Desai T and Bhatia S) pp 95–123, Springer US.

http://www.springer.com/978-0-387-98119-2

Implantable Neural Prostheses 2
Techniques and Engineering Approaches
(Eds.)D. Zhou; E. Greenbaum
2010, XIII, 371 p. 189 illus., 61 in color., Hardcover
ISBN: 978-0-387-98119-2